




PRECLINICAL REPORTS

Assessment of a 3050/3200 nm fiber laser system for ablative fractional laser treatments in dermatology

Michael Wang-Evers PhD¹  | Alyre J. Blazon-Brown BSc¹ |
Linh Ha-Wissel MD, MSc^{1,2}  | Valeriya Arkhipova PhD, Dr rer nat³  |
Dilip Paithankar PhD⁴ | Ilya V. Yaroslavsky PhD⁴ | Gregory Altshuler PhD⁴ |
Dieter Manstein MD, PhD¹

¹Department of Dermatology, Cutaneous Biology Research Center, Massachusetts General Hospital, Harvard Medical School, Boston, Massachusetts, USA

²Department of Dermatology, Allergology and Venereology, University Hospital Schleswig-Holstein, Lübeck, Germany

³NTO IRE-Polus, Fryazino, Russia

⁴IPG Medical, IPG Photonics Corporation, Marlborough, Massachusetts, USA

Correspondence

Michael Wang-Evers, Department of Dermatology, Cutaneous Biology Research Center, Massachusetts General Hospital, Harvard Medical School, Charlestown, MA, USA.
Email: mevers@mgh.harvard.edu

Abstract

Background and Objectives: Mid-infrared (IR) ablative fractional laser treatments are highly efficacious for improving the appearance of a variety of dermatological conditions such as photo-aged skin. However, articulated arms are necessary to transmit the mid-IR light to the skin, which restricts practicality and clinical use. Here, we have assessed and characterized a novel fiber laser-pumped difference frequency generation (DFG) system that generates ablative fractional lesions and compared it to clinically and commercially available thulium fiber, Erbium:YAG (Er:YAG), and CO₂ lasers.

Materials and Methods: An investigational 20 W, 3050/3200 nm fiber laser pumped DFG system with a focused spot size of 91 μm was used to generate microscopic ablation arrays in ex vivo human skin. Several pulse energies (10–70 mJ) and pulse durations (2–14 ms) were applied and lesion dimensions were assessed histologically using nitro-blue tetrazolium chloride stain. Ablation depths and coagulative thermal damage zones were analyzed across three additional laser systems.

Results: The investigational DFG system-generated deep (>2 mm depth) and narrow (<100 μm diameter) ablative lesions surrounded by thermal coagulative zones of at least 20 μm thickness compared to 13, 40, and 320 μm by the Er:YAG, CO₂, and Thulium laser, respectively.

Conclusion: The DFG system is a small footprint device that offers a flexible fiber delivery system for ablative fractional laser treatments, thereby overcoming the requirement of an articulated arm in current commercially available ablative lasers. The depth and width of the ablated microcolumns and the extent of surrounding coagulation can be controlled; this concept can be used to design new treatment procedures for specific indications. Clinical improvements and safety are not the subject of this study and need to be explored with in vivo clinical studies.

KEYWORDS

difference frequency generation, fiber delivery, fractional ablation, fractional laser

BACKGROUND

Selective photothermolysis (SP) describes the dependence of tissue interactions on the laser wavelength, pulse duration, and pulse energy for particular chromophore targets.¹ The theory suggests that to obtain permanent thermal damage (thermolysis) of a target, laser light must be absorbed by the target and energy must be confined to the targeted structure, the latter keeping surrounding tissue intact, by keeping the pulse duration shorter than the thermal relaxation time.² Compared to hemoglobin or melanin, water is not a useful target for SP since it is present at a high concentration throughout the skin (approximately 60%–80% of the epidermis and dermis).³ To target water as a chromophore and to avoid bulk heating of the skin, fractional photothermolysis (FP) was invented.⁴ In FP, short laser pulses with high peak fluences focused into small spots create spatially separated microscopic damage zones, leaving surrounding areas of skin perfectly intact. While SP relies on selective absorption of pigmented target structures and FP relies on optical foci within a largely uniform medium, both cause small, spatially limited zones of photothermal effects within the tissue.⁴

Traditionally, fully ablative laser resurfacing treatments with Erbium:YAG (Er:YAG) (2.94 μm) and CO₂ (10.6 μm) lasers were used to remove the top layer of skin (epidermis and superficial or papillary dermis) in a uniform way. This technique achieves excellent improvement for numerous dermatological conditions, but with the risk of adverse events such as pigmentary changes and significant social downtime during which patients have to endure oozing, crusting, and erythema that usually lasts between 1 and 4 weeks depending on the parameters chosen.⁵ Multiple successive fractional laser treatments (applying the concept of FP) have been shown to achieve similar clinical outcomes as fully ablative laser resurfacing, but with fewer adverse events and lower downtimes, in the range of 3–5 days after each treatment.^{4–6} Such treatment of the skin in fractions has been done with both nonablative fractional lasers (NAFLs) and ablative fractional lasers (AFLs). NAFLs produce microscopic coagulation zones, while AFLs generate microscopic ablation zones (MAZs) of controlled width, depth, and densities. Based on the water absorption coefficient μ_a , wavelengths of the near- to mid-infrared spectrum (1064–1940 nm, $\mu_a < 130 \text{ cm}^{-1}$) are suitable for NAFL treatments, whereas wavelengths of the mid-infrared spectrum (1940–10600 nm, $\mu_a > 130 \text{ cm}^{-1}$) are used for AFL treatments.⁷ There is a transitional range of wavelengths around 1940 nm suitable for both, AFL and NAFL treatments depending on the laser energy density and focused spot size. Both AFL and NAFL systems produce arrays of ablation and/or coagulative thermal damage surrounded by undamaged skin,

which allows fast epidermal repair and have been successfully used for improving the appearance of scars, epidermal pigmentation, melasma, and photo-damaged skin.^{8–11}

There are three modalities with which fractional laser energy can be delivered from the laser output to the tissue: the first is an articulated arm with a system of reflecting mirrors, the second is a solid core fiber, and the third is a hollow waveguide. The most commonly used delivery system of AFLs such as Er:YAG and CO₂ lasers is the articulated arm.¹² However, there exist several downsides with these systems, such as constrained flexibility and ridged movement of the arm during procedures. Additionally, articulated arms can get misaligned when not handled properly or during transport, which can cause beams to wander and require expensive maintenance by a specialist. Therefore, efforts have been made to find alternative delivery systems that are lightweight and highly flexible such as fiber delivery systems. Fiber delivery addresses the aforementioned problems and fundamentally increases the practicality of lasers in dermatology.

Compared to articulated arms, fiber delivery systems use solid core fibers. These fibers made out of silica are common and inexpensive, but silica strongly absorbs wavelengths $> 2.1 \mu\text{m}$, and therefore cannot be used for the delivery of mid-infrared light employed in AFL systems.¹³ Other solid core fiber materials for wavelengths $> 2.1 \mu\text{m}$ exist (e.g., sapphire), but are not suitable for mass applications.¹⁴ Hence, solid core fiber delivery is currently limited for use in NAFL systems at wavelengths $< 2.1 \mu\text{m}$.

In addition to articulated arms and solid-core fibers, hollow waveguides have been investigated as an option to deliver mid-infrared laser light for medical applications.¹⁴ While hollow IR-transmitting waveguides do offer an alternative to solid-core fibers in high-power laser delivery applications, the hollow structure makes them fragile and does not allow for tight bends as this would break the waveguide. Due to this concern, hollow waveguides have not reached broad uptake in clinical practices.

Even though AFLs are an effective treatment for facial rejuvenation, the lack of reliable and cost-effective means of guiding optical power in an optical fiber or other flexible delivery systems limits the practicality and scope of dermatological applications significantly. In this study, we assess a novel ablative fractional fiber laser-pumped DFG system that allows flexible fiber delivery for dermatological applications. The prototype DFG system has two highly water absorbed output wavelengths (3050 and 3200 nm) and it generates large peak radiant exposures, which allow for narrow and controlled depth ablations in the skin. Here, we show for the first time MAZs in human ex vivo skin with a novel ablative fiber laser-pumped DFG system, which were analyzed and compared to histological outcomes of

clinical and commercially available laser systems such as Thulium, Er:YAG, and CO₂ lasers. We anticipated and verified significant differences in ablation depth and thermal damage between these lasers, based on the laser parameters, and water absorption properties. Furthermore, we discuss the suitability of this prototype system for clinical applications.

MATERIALS AND METHODS

Laser systems

Laser pulse exposures on skin tissue were performed with a commercially available Thulium fiber laser, a clinical Er:YAG laser, a prototype fiber laser pumped DFG system, and a clinical CO₂ laser. The laser pulse properties are summarized in Table 1. The focused spot size, Rayleigh range, and beam quality factor M^2 were experimentally determined with the knife-edge technique for each laser system.¹⁵

Thulium fiber laser (1940 nm)

A thulium fiber laser (TLR-120-1940; IPG Photonics Corporation) was gated to generate 2–7 ms pulses with a rectangular-shaped temporal pulse structure. The Thulium fiber laser beam was focused on a 108- μ m beam diameter and radiant exposures of 872–8986 J/cm² (80, 101, 126, 157, 185, 194, 212, 488, and 854 mJ/pulse) were used.

Er:YAG laser (2940 nm)

A clinical ablative fractional Er:YAG laser (Sciton Profile; Sciton Inc.) was used to treat ex vivo human tissue. Laser microspots were delivered in 250 μ s pulses, with a spot size of 256 μ m and a 10% treatment density at radiant exposures of 51–306 J/cm² (25, 50, ..., 150 mJ/pulse).

Fiber laser pumped DFG (3050/3200 nm)

The DFG system (IPG Photonics Corporation) is a novel, small footprint, tabletop system that consists of a base unit, a flexible umbilical cord, and a handpiece (Figure 1). The base unit consists of two diode-pumped fiber lasers, namely, a 1030-nm ytterbium-doped pump fiber laser and a 1560-nm Er seed fiber laser. A multimode fiber delivers these wavelengths to the handpiece where they are combined in a two-stage nonlinear crystal converter to generate 3050 and 3200 nm wavelengths via the difference frequency generation (DFG) process (Figure 2).^{16,17} The ratio of emitted wavelengths for 3050 versus 3200 nm is approximately 2:1. Both wavelengths are collimated onto a scanner mirror in the handpiece and focused on skin with free-space optics to a spot size of 91 μ m. The 1030 and 1560 nm laser light is returned to the base unit via another optical fiber and dumped into a beam trap. The system produces 2–20 ms pulses, which consists of a train of 2 ns full-width at half-maximum (FWHM) pulse duration nanoseconds. Pulses with energies of 10, 20, ...70 mJ

TABLE 1 Laser wavelength, beam diameter, pulse energy, and other parameters for the four laser systems tested in this study

Model	Thulium fiber TLR-120-1940	Er:YAG Sciton Profile	DFG Prototype	CO ₂ UltraPulse
Manufacturer	IPG Photonics	Sciton	IPG Photonics	Lumenis Ltd.
Wavelength λ (nm)	1940	2940	3050/3200	10600
Absorption coefficient μ_a (cm ⁻¹)	135	12,800	9990/3630	1000
Optical penetration depth δ (μ m)	74.1	0.8	1/2.8	10
Beam diameter $2\omega_0$ (μ m)	108	256	91	120
Pulse energy E_p (mJ)	80–854	25–150	10–70	20–132
Radiant exposure H_0 (J/cm ²)	872–2310	51–306	154–1076	177–1166
Rayleigh range z_0 (mm)	3.37	1.92	1.68	0.82
Pulse width τ (ms)	2–7	0.25	1–20	1
Thermal confinement (ms)	9.6	0.001	0.002/0.014	0.17
Stress confinement (ns)	48.1	0.5	0.6/1.8	6.5
Beam quality factor M^2	1.4	9.1	1.2	1.3

Abbreviations: DFG, difference frequency generation; Er:YAG, erbium:YAG.

corresponding to radiant exposures in the range of 154–1076 J/cm² were used.

CO₂ laser (10600 nm)

A clinical fractional CO₂ laser system (UltraPulse; Lumenis Ltd.) was used. The emitted laser pulse is composed of a 1-ms train of micro-oscillations with a repetition frequency of 2 MHz (220 ns FWHM micropulses). The DeepFX handpiece provided a focal spot diameter of 120 μm and radiant exposures of 177–1165 J/cm² (20, 43, 70, 85, 110, 117, and 132 mJ/pulse) were applied.

Preparation, treatment, and analysis of ex vivo skin

Full-thickness frozen ex vivo abdominal human skin samples were cleaned of fat, fascia, and hair. Thawed



FIGURE 1 Photograph of the prototype ablative fractional fiber laser pumped DFG system. The small footprint base unit has output wavelengths of 1030 and 1560 nm, which are fiber delivered to a scanner handpiece. The scanner handpiece contains DFG crystals that convert the laser light wavelength to 3050 and 3200 nm (ratio of 2:1). DFG, difference frequency generation.

tissue samples were pinned onto polystyrene foam boards with the epidermal side facing up at 32°C temperature. Depending on the laser system, tissue ablation arrays were generated by scanning systems or manually by a micrometer translation stage. Exposed tissue samples were embedded in optimal cutting temperature compound (Tissue-Tek OCT) and 20-μm-thick vertical sections were obtained by continuous cryosectioning. Sections were stained with nitro-blue tetrazolium chloride (NBTC), a lactate dehydrogenase activity stain to assess the extent of thermally induced damage,¹⁸ and analyzed using a digital slide scanner (NanoZoomer S60; Hamamatsu). The ablation depth was defined as the maximum channel depth of ablated lesions. The coagulation zone thickness and laser channel diameter were measured at the top (10%–30%) of the ablated lesion. Tissue ablations of 1 mm depth generated by each laser system were compared to each other (thulium: 854 mJ pulse energy and 7 ms pulse width, Er:YAG: 50 mJ pulse energy and 0.25 ms pulse width, DFG: 20 mJ pulse energy and 4 ms pulse width, CO₂: 40 mJ pulse energy and 1 ms pulse width). At least five individual lesions for each setting were analyzed and average values of ablation depth, channel diameter, and coagulation zone thickness were determined.

Thermal and stress confinement

Due to differences in the laser wavelength, focused beam size, pulse duration, optical penetration depth δ , and heat conduction of the deposited energy, the propagation of thermoelastic stresses differ significantly across the four laser systems used in this study. Spatially confined effects of heat conduction can be achieved by using laser pulse durations that are shorter than the thermal diffusion time τ_d of the heated volume.¹ For laser ablation in soft tissue where the optical penetration depth is smaller than the focused beam size, the heated volume can be approximated by a planar layer, and the characteristic thermal diffusion time is given as:

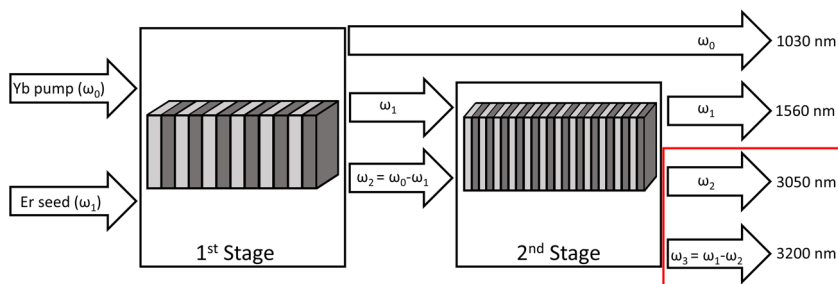


FIGURE 2 Two-stage conversion setup scheme. Each stage consists of a periodically poled lithium niobate crystal that generates light with an output frequency that is the difference between the two input frequencies according to the DFG process. Image adapted from Gulyashko et al.¹⁶ DFG, difference frequency generation; Er, erbium; Yb, ytterbium.

$$\tau_d = \frac{\delta^2}{\kappa}, \quad (1)$$

where $\kappa = 1.43 \times 10^{-3} \text{ cm}^2/\text{seconds}$ is the thermal diffusivity of water.¹⁹ In addition to rapid and confined heating, short-pulse laser irradiation of tissue leads to the generation and propagation of thermoelastic stresses. The stress confinement time τ_s is the time a stress wave needs to traverse through the directly heated volume of the tissue²⁰:

$$\tau_s = \frac{\delta}{c_a}, \quad (2)$$

where $c_a = 1540 \text{ m/seconds}$ is the speed of sound in soft biological tissue.²¹ When stress confinement conditions are fulfilled, the ablation process results in an increase in ablation efficiency and a decrease in thermal coagulation zones.²² Table 1 shows laser system-dependent parameters like wavelength and penetration depth, as well as the thermal confinement time and stress confinement time of water. It is important to highlight that human tissue has water contents from 15%–30% (stratum corneum) to 60%–80% (epidermis and dermis) and that the absorption coefficient also depends on temperature.^{3,23}

Laser ablation threshold and models

The laser ablation threshold of tissue determines the minimum required radiant exposure to achieve ablative material removal.²⁴ Different models have been proposed to characterize and predict outcomes of laser ablation processes like the amount of removed material.²⁵ There are two fundamental ablation models, describing the extreme cases of absence of thermal diffusion (“blow-off” model) and thermal steady-state conditions (“steady-state” model). Both ablation models simplify the laser–tissue interaction and have been described in other work in detail.^{26,27} In short, the blow-off model assumes that a minimum threshold radiant exposure H_{th} is required to initiate ablation.²⁰ Radiant exposures below the ablation threshold only result in heating of the target. The model assumes that conditions for thermal confinement are satisfied. The model shows a semi-logarithmic relationship between the ablation depth δ_{abl} and the incident radiant exposure H_0 ²²:

$$\delta_{abl} = \frac{1}{\mu_a} \ln \left(\frac{H_0}{H_{th}} \right). \quad (3)$$

The steady-state model predicts that material removal occurs during the irradiation of the tissue linearly with time. It is used for microsecond and millisecond laser pulses. Compared to the blow-off model, it assumes a linear relationship between ablation depth and radiant exposure²²:

$$\delta_{abl} = \frac{H_0 - H_{th}}{\mu_a H_{th}}. \quad (4)$$

To unify the logarithmic blow-off model and the linear steady-state model, we can use the Hibst model^{27,28}:

$$\delta_{abl} = \frac{1}{\mu_a \gamma} \ln \left(\gamma \frac{H_0}{H_{th}} - \gamma + 1 \right), \quad (5)$$

where γ is used as a parameter to approximate whether an ablation process is closer to the blow-off model ($\gamma \rightarrow 1$) or to the steady-state model ($\gamma \rightarrow 0$). The data are analyzed with the three models described above.

RESULTS

Laser–tissue interaction

As expected, the ablation depths grew in size with increasing radiant exposures and were comparatively greater for laser systems with higher absorption coefficients (Figure 3). It was also anticipated that the ablation depth slope would increase with rising water absorption coefficients (Figure 3). Thulium laser ablation even at high radiant exposure was only superficial; this was a result of the high ablation threshold (Table 2) and low water absorption coefficient. The ablation channel diameter was smallest for the DFG system ($92 \pm 8 \mu\text{m}$), followed by the CO₂ laser ($138 \pm 12 \mu\text{m}$), the Thulium laser ($146 \pm 15 \mu\text{m}$), and the Er:YAG laser ($252 \pm 16 \mu\text{m}$), which agrees with the knife-edge measured focal spot sizes in Table 1. The Thulium laser created slightly oval ablation craters (short:long axis ratio, 1:1.3), while the other laser systems led to circular craters.

Coagulative thermal damage

The coagulative damage at the edges of the ablation crater is consistent in size and it increases with higher optical penetration depths (lower absorption coefficient) shown in Figure 4. Therefore, the largest coagulation zones were generated by the Thulium laser followed by the CO₂ laser, the DFG system, and then the Er:YAG laser. For the Thulium laser, thermal confinement is satisfied (Equation 1), meaning that the laser efficiently removes tissue and that a reduction in thermal damage can only be achieved by reducing the pulse duration to also fulfill stress confinement conditions (Equation 2). The Er:YAG laser, DFG system, and CO₂ laser could theoretically achieve smaller coagulation zones by reducing the pulse duration until thermal or stress confinement conditions are fulfilled (Table 1). However, due to the high water absorption coefficients of these

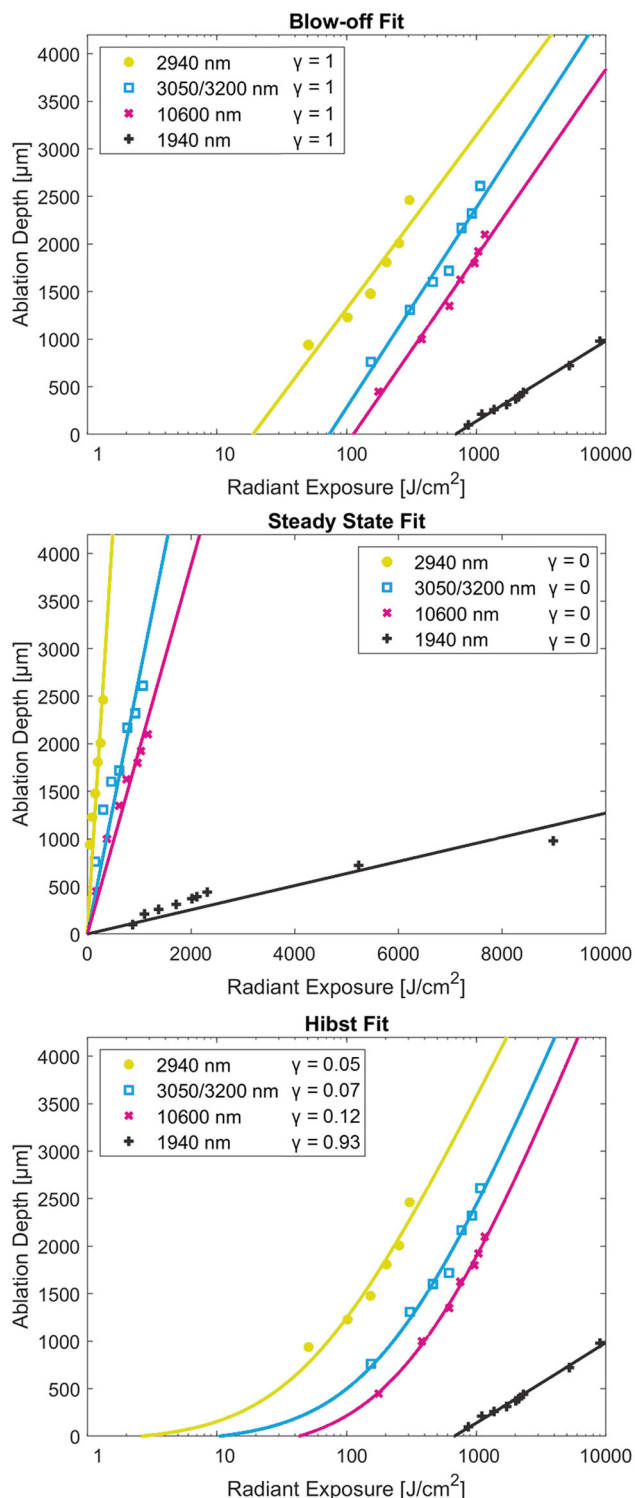


FIGURE 3 Blow-off, steady-state, and Hibst models to fit the ablation depth versus radiant exposure curves of the Er:YAG (2940 nm), fiber laser-pumped DFG (3050/3200 nm), CO₂ (10600 nm), and Thulium (1940 nm) laser in ex vivo human tissue. The Hibst model (with the extra adjustable parameter γ) results in a better fit for every wavelength compared to the blow-off and steady-state model. DFG, difference frequency generation; Er, erbium.

laser system wavelengths, thermal coagulation times are in the microsecond range and stress confinement times are in the few nanosecond range (Table 1), and therefore, none of the laser–tissue experiments fulfilled these conditions. Here, the smallest experimental achievable coagulation zone of the Er:YAG laser was $12 \pm 4 \mu\text{m}$, while the DFG system, CO₂, and Thulium laser were limited to larger coagulation depths of 20 ± 5 , 40 ± 11 , and $320 \pm 32 \mu\text{m}$.

Ablation metrics

The parameters (H_{th} and γ) in Equations (3), (4), and (5) were fit with a nonlinear least-squares fitting algorithm (lsqcurvefit, Matlab2019b; MathWorks) to the experimental data and the resulting values are summarized in Table 2. For the blow-off and the Hibst model, the experimentally determined ablation thresholds in tissue were significantly higher than the theoretically determined thresholds for water evaporation for each wavelength. The steady-state fit for the experimental data can be neglected since it resulted in ablation thresholds of 0 J/cm^2 for each wavelength. This can be explained by the simplicity and the linear nature of the steady-state model, which fails to adequately fit logarithmic data. The Thulium laser can be best described by the Hibst model with a γ parameter of 0.93 (Table 2). The Er:YAG, DFG system, and CO₂ laser are best described by the Hibst model with γ parameters of 0.05, 0.07, and 0.12, respectively.

Pulse duration

Figure 5 shows that ablation and coagulation depth can be modulated by varying the laser pulse duration. While the pulse duration of the clinical Er:YAG and CO₂ laser systems could not be varied, it has been previously shown that the coagulation zone thickness of these systems can be modulated.²⁹ However, the minimum coagulation zone thickness is limited by the optical penetration depths (inversely dependent on the water absorption coefficient) at each laser wavelength. While the coagulation width increases via heat diffusion, it cannot be reduced below the optical penetration depth. This theoretical coagulation depth (optical penetration depth) is the smallest for the Er:YAG laser, followed by the DFG system, the CO₂ laser, and the Thulium laser (Table 2). By adjusting the laser parameters, the Er:YAG laser and DFG system allow for the largest range of coagulation depth control and are suitable for treatments that require a range of coagulation depths. The CO₂ and Thulium laser, however, are confined by their minimum coagulation depth which is significantly larger.

TABLE 2 Theoretical ablation threshold (H_{th}) of water (70%) and experimentally determined ablation thresholds of ex vivo human skin using the blow-off, steady-state, and Hibst models for the Thulium, Er:YAG, DFG, and CO₂ laser

	70% Water H_{th} (J/cm ²)	Blow-off model		Steady-state model		Hibst model		
		H_{th} (J/cm ²)	R^2	H_{th} (J/cm ²)	R^2	H_{th} (J/cm ²)	γ	R^2
Thulium fiber	26.8	689.6	0.991	0	0.833	676.3	0.93	0.992
Er:YAG	0.3	18.9	0.901	0	0.694	2.7	0.05	0.944
DFG	0.4/1	73.5	0.964	0	0.752	10.4	0.07	0.981
CO ₂	3.6	112.6	0.985	0	0.917	42.9	0.12	0.996

Note: R^2 is the square of Pearson's correlation coefficient, which is a measure of how well the model predictions and the experimental data match with each other. Abbreviations: DFG, nitro-blue tetrazolium chloride; Er, erbium.

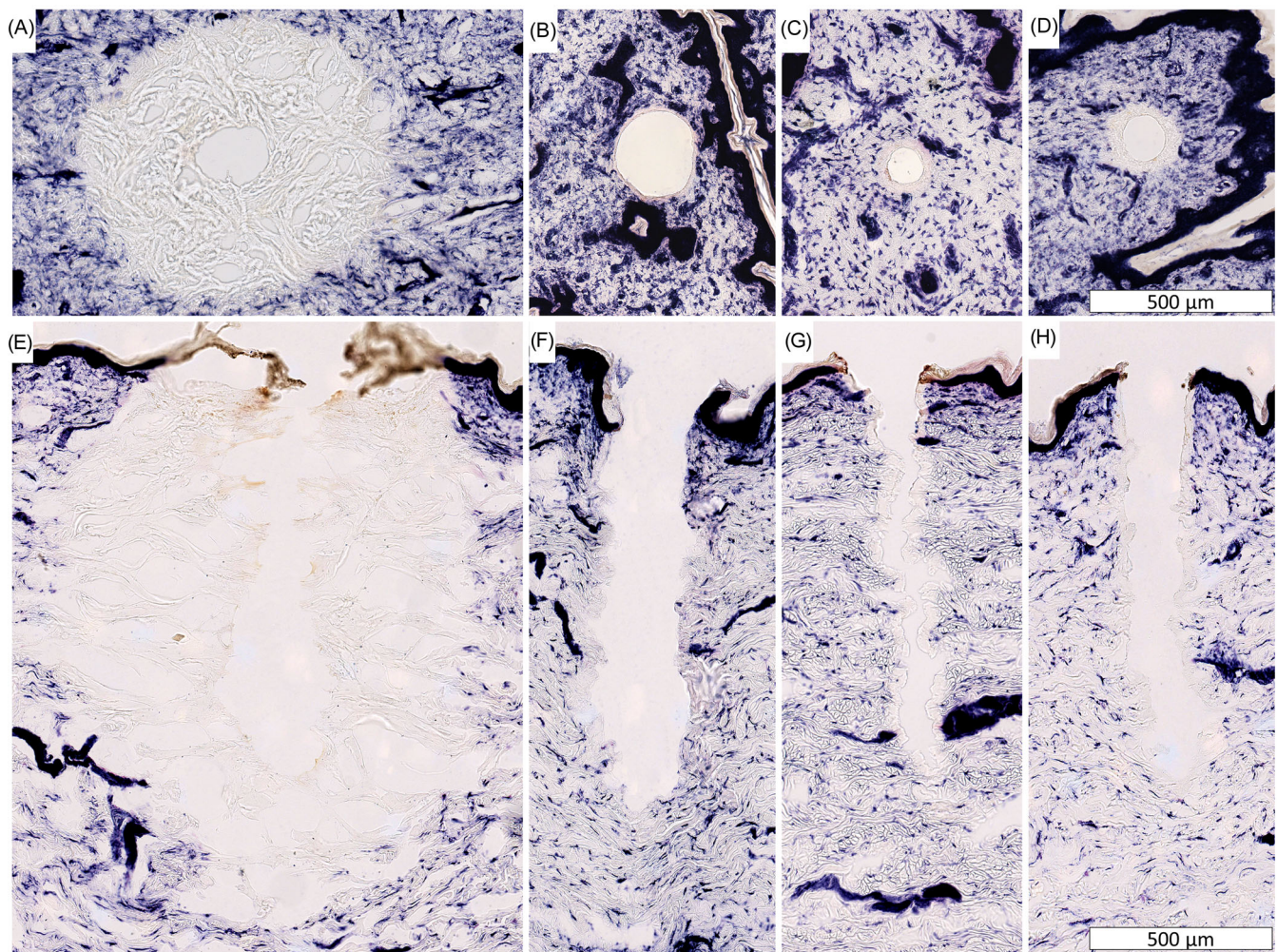


FIGURE 4 Horizontal histology sections of ex vivo human skin treated with (A) Thulium, (B) Er:YAG, (C) fiber laser pumped DFG, and (D) CO₂ laser stained with NBTC. For corresponding vertical histology sections below (E–H) laser parameters were chosen to generate 1-mm-deep ablated fractional lesions. The horizontal sections show clear differences in the size of the coagulation zone. The Thulium laser parameters are 108 μm spot size, 854 mJ pulse energy, 7 ms pulse width, and 1940 nm wavelength. The Er:YAG laser parameters are 250 μm spot size, 50 mJ pulse energy, 0.25 ms pulse width, and 2940 nm wavelength. The fiber laser-pumped DFG parameters are 91 μm spot size, 20 mJ pulse energy, 4 ms pulse width, and 3050/3200 nm wavelength. The CO₂ laser parameters are 120 μm spot size, 40 mJ pulse energy, 1 ms pulse width, and 10600 nm wavelength. DFG, difference frequency generation; Er, erbium; NBTC, nitro-blue tetrazolium chloride.

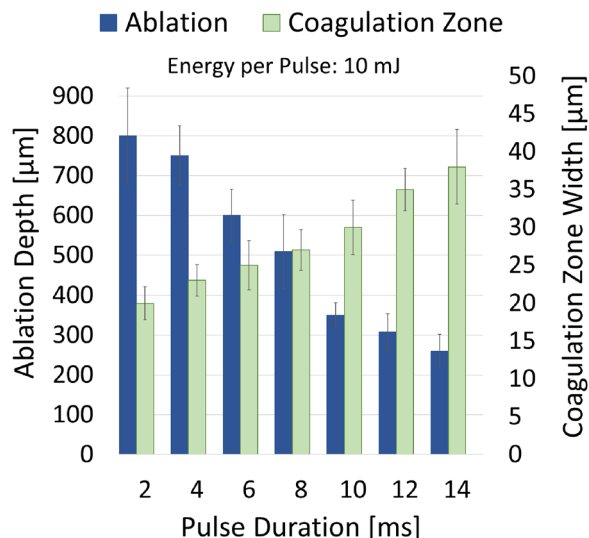


FIGURE 5 The graph shows the effect of the pulse train duration on the ablation depth and coagulation zone thickness in ex vivo human tissue using the fiber laser-pumped DFG. The energy per pulse stays constant at 10 mJ (radiant exposure of 154 J/cm²) for the pulse train duration of 2, 4, 6, 8, 10, 12, and 14 ms. DFG, difference frequency generation.

DISCUSSION

AFLs are considered the gold standard for many low-downtime dermatological treatments and numerous studies have been published on the excellent clinical effects, especially when used on the face.^{5,8,30} The DFG system used in this study has wavelengths and water absorption coefficients between the most commonly used clinical lasers (Er:YAG and CO₂) and our results showed that its ablation efficiency is comparable with both systems. To circumvent the need for an articulated arm, several AFL systems have been developed where laser components such as flashlamp, laser crystal, and so on can be found inside the handpiece.⁶ While these laser systems avoid using articulated arms, their handpieces are often heavy, bulky, require water cooling, and have fixed scanning patterns.^{31,32} Here, the DFG system converts the fiber delivered pump laser light inside the handpiece making it lightweight and flexible. Additionally, the DFG handpiece contains a laser scanner that allows for a variety of scan patterns and densities.

One of the goals of this study was to determine the residual coagulative thermal damage around the ablated lesions of each of the four laser systems as it determines the wound healing process and clinical outcome.³³ Currently, the Thulium laser is the only commercially available fiber-delivered system that could be used for AFL treatments. However, excessive thermal coagulation zones presented in Figure 4 would most likely result in adverse effects such as scarring, making the device unsuitable for in vivo experiments and clinical practice. In comparison, the thermal damage caused by the DFG

system makes us believe that it is sufficient to provide new collagen formation in the dermis while maintaining a short wound healing time similar to that of Er:YAG laser treatments. Currently, fractional Er:YAG treatments produce significant oozing and bleeding when generating ablation depths beyond 500 μm, because they generate minimal tissue coagulation (larger coagulation zones help in minimizing bleeding).³⁴ Compared to that, CO₂ lasers produce less oozing, greater collagen remodeling, and better efficacy for the treatment of facial rhytids, but are associated with higher intra-operative and post-operative pain and have a greater risk of complications such as hypopigmentation and scarring due to larger thermal coagulation zones.^{35,36} The DFG system could produce a better blend of coagulation and ablation than the CO₂ and Er:YAG laser, similar to the laser-tissue interaction of less commonly used Er:YSGG lasers (2790 nm) or Er:YAG laser systems that are capable of producing a train of subpulses to increase the degree of thermal coagulation.^{6,35}

Another part of this study was to analyze and characterize each system's laser-tissue interaction. Therefore, the relationship between ablation depth and radiant exposure was determined and described by simple heuristic ablation models. The Thulium laser ablation curve was best fitted by the blow-off ($\gamma \rightarrow 1$) and Hibst model ($\gamma = 0.93$), which conforms with the ablation characteristics found in literature and allows for a rapid, albeit rough estimation of the ablation depth.²⁷ The γ values of the Er:YAG, DFG, and CO₂ laser systems were close to zero (0.05, 0.07, and 0.12, respectively), suggesting a steady state-like relationship between ablation rate and incident energy. However, the linear steady-state fit is not applicable since it is a simple approximation, which does not include any of the attenuation and energy losses that can occur such as shielding effects by ejected materials, tissue shrinkage, and other nonlinear effects.²⁶ Therefore, the more sophisticated Hibst model resulted in the best approximation of our experimental data, even though it produced ablation thresholds that were several times larger than the theoretically determined thresholds for water evaporation (Table 1). This was expected since skin is a heterogeneous material with different water contents and mechanical strength for each layer, which results in higher ablation thresholds compared to water.²² Despite the applicability issues mentioned above, the Hibst model provides a basic understanding of the energetics of thermal ablation processes and allows for an approximation of the ablation depth and threshold.

For the clinical outlook, we have shown that the fractional DFG system results in a greater zone of coagulation compared to Er:YAG lasers, and we, therefore, hypothesize that it might produce less bleeding and better dermal collagen remodeling. The DFG system presents less thermal coagulation than CO₂ lasers, resulting in more controlled thermal heating with

potentially less risk for scarring and long-term dyspigmentation.⁶ The DFG system's capability of creating coagulation zones of different sizes (20–40 μm) could be advantageous for laser-assisted drug delivery where thick coagulation zones can restrict the diffusion of large drug molecules; however, if sized correctly, the thermal damage zone can act as a reservoir to provide a slow release of the drug to the surrounding dermis.³⁷

Additionally, by varying the radiant exposure of the DFG system, the ablated lesion depth in the skin is tunable and could be adjusted for specific treatments such as reduction of undesired superficial wrinkles, pigmentation, or scars.^{7,8} Further, most fractional Er:YAG lasers operate in the multimode regime, which makes the output beam highly divergent and of low quality ($M^2 = 9.1$) and therefore reduces the potential for diffraction-limited focused spot sizes.³⁸ The DFG system, on the other hand, has great beam quality ($M^2 = 1.2$), which allows for close to diffraction-limited focal spot sizes. If desired, future iterations of the DFG system could further reduce the focused spot size of currently 91 μm to below 50 μm . This could potentially lead to new dermatological applications that require narrow ablation channels as well as reduce wound healing times. Further, the large Rayleigh length of the Er:YAG and DFG systems compared to the CO₂ laser (Table 1) reduces the clinical impact of deviations from the focal plane, which could improve the safety and efficacy of ablative fractional resurfacing procedures.³⁹

The limitations of this study are intrinsic to ex vivo human skin experiments, specifically the availability and quality of the tissue. While most dermatological laser applications are performed in facial tissue, our experiments were performed in previously frozen human abdominal skin from Caucasian women of older age. Additionally, there is a difference in ex vivo and in vivo conditions in terms of blood circulation, which may cause bleeding and changes in laser absorption as well as heat distribution. Despite these limitations, our current histologic findings provide the basis for future clinical studies and highlight that the DFG system is a promising platform for AFL applications.

CONCLUSIONS

We characterized the ablation and coagulation capabilities of a novel flexible fiber laser-pumped DFG and compared it to commercially available Thulium fiber, Er:YAG, and CO₂ lasers. The wavelengths of the DFG system are highly absorbed by water and generate deep ablated lesions with a minimum coagulative thermal damage zone that is two times larger than that of the Er:YAG laser and half the size as compared to CO₂ lasers. For each laser system, we have described the laser–tissue interaction with simplified heuristic ablation models and found a close correspondence of the DFG

system with the Er:YAG and CO₂ lasers. Besides efficient soft tissue ablation, the DFG system produces ablated laser lesions that are surrounded by coagulation zones whose width can be adjusted. In addition, to the best of our knowledge, the DFG device is the first fiber-delivered system suited for AFL treatments that overcome the need for articulated arms of presently used AFLs. While ex vivo studies are appropriate for the analysis of laser–tissue interaction, in vivo clinical studies will be required for the investigation of various indications.

ACKNOWLEDGMENTS

We would like to thank William “Bill” Farinelli and Rox Anderson for providing support and access to the Er:YAG laser. The Thulium fiber laser and DFG system were provided by IPG Photonics as a loaner free of charge to the laboratory. The CO₂ laser was a gift provided by Lumenis Ltd.


CONFLICTS OF INTEREST

The authors declare no conflicts of interest.

ORCID

Michael Wang-Evers  <https://orcid.org/0000-0002-6461-4891>

Linh Ha-Wissel  <https://orcid.org/0000-0002-7641-9647>

Valeriya Arkhipova  <https://orcid.org/0000-0002-7304-6267>

REFERENCES

- Anderson R, Parrish J. Selective photothermolysis: precise microsurgery by selective absorption of pulsed radiation. *Science*. 1983;220(4596):524–7.
- Altshuler GB, Anderson RR, Manstein D, Zenzie HH, Smirnov MZ. Extended theory of selective photothermolysis. *Lasers Surg Med*. 2001;29(5):416–32.
- Kourbaj G, Bielfeldt S, Seise M, Wilhelm K-P. Measurement of dermal water content by confocal RAMAN spectroscopy to investigate intrinsic aging and photoaging of human skin in vivo. *Skin Res Technol*. 2021;27(3):404–13.
- Manstein D, Herron GS, Sink RK, Tanner H, Anderson RR. Fractional photothermolysis: a new concept for cutaneous remodeling using microscopic patterns of thermal injury. *Lasers Surg Med*. 2004;34(5):426–38.
- You H-J, Kim D-W, Yoon E-S, Park S-H. Comparison of four different lasers for acne scars: resurfacing and fractional lasers. *J Plast Reconstr Aesthet Surg*. 2016;69(4):e87–95.
- Dierickx CC, Khatri KA, Tannous ZS, Childs JJ, Cohen RH, Erofeev A, et al. Micro-fractional ablative skin resurfacing with two novel erbium laser systems. *Lasers Surg Med*. 2008;40(2):113–23.
- Bodendorf MO, Grunewald S, Wetzig T, Simon JC, Paasch U. Fractional laser skin therapy. *J Dtsch Dermatol Ges*. 2009;7(4):301–8.
- Waibel JS, Gianatasio C, Rudnick A. Randomized, controlled early intervention of dynamic mode fractional ablative CO₂ laser on acute burn injuries for prevention of pathological scarring. *Lasers Surg Med*. 2020;52(2):117–24.
- Wong CSM, Chan MWM, Shek SYN, Yeung CK, Chan HHL. Fractional 1064 nm picosecond laser in treatment of melasma and skin rejuvenation in Asians, A prospective study. *Lasers Surg Med*. 2021;53(8):1032–42.

10. Passeron T, Genedy R, Salah L, Fusade T, Kosiratna G, Laubach HJ, et al. Laser treatment of hyperpigmented lesions: position statement of the European Society of Laser in Dermatology. *J Eur Acad Dermatol Venereol*. 2019;33(6):987–1005.
11. Casper MJ, Glahn J, Evers M, Schulz-Hildebrandt H, Kosiratna G, Birngruber R, et al. Capillary refill—the key to assessing dermal capillary capacity and pathology in optical coherence tomography angiography. *Lasers Surg Med*. 2020;52(7):653–8.
12. Shokrollahi K, Raymond E, Murison MSC. Lasers: principles and surgical applications. *J Surg*. 2004;2(1):28–34.
13. Humbach O, Fabian H, Grzesik U, Haken U, Heitmann W. Analysis of OH absorption bands in synthetic silica. *J Non-Cryst Solids*. 1996;203:19–26.
14. Verdaasdonk RM, Swol CFPv. Laser light delivery systems for medical applications. *Phys Med Biol*. 1997;42(5):869–94.
15. de Araújo MA, Silva R, de Lima E, Pereira DP, de Oliveira PC. Measurement of Gaussian laser beam radius using the knife-edge technique: improvement on data analysis. *Appl Opt*. 2009;48(2):393–6.
16. Gulyashko AS, Larionov IA, Tyrtshnyy VA. Optimization of the efficient single pass two-stage DFG of Er and Yb fiber lasers radiation into mid-infrared region. Paper presented at 2019 Conference on Lasers and Electro-Optics Europe & European Quantum Electronics Conference (CLEO/Europe-EQEC); 2019 Jun 23–27.
17. Pandey AR, Powers PE, Haus JW. Experimental performance of a two-stage periodically poled lithium niobate parametric amplifier. *IEEE J Quantum Electron*. 2008;44(3):203–8.
18. Chung J-H, Koh W-S, Youn J-I. Histological responses of port wine stains in brown skin after 578 nm copper vapor laser treatment. *Lasers Surg Med*. 1996;18(4):358–66.
19. Valvano JW. Tissue thermal properties and perfusion. In: Welch AJ, Van Gemert MJC, editors. *Optical-thermal response of laser-irradiated tissue*. Boston: Springer US; 1995. p. 445–48.
20. Walsh JT, Cummings JP. Effect of the dynamic optical properties of water on midinfrared laser ablation. *Lasers Surg Med*. 1994;15(3):295–305.
21. Shin HC, Prager R, Gomersall H, Kingsbury N, Treece G, Gee A. Estimation of average speed of sound using deconvolution of medical ultrasound data. *Ultrasound Med Biol*. 2010;36(4):623–36.
22. Vogel A, Venugopalan V. Mechanisms of pulsed laser ablation of biological tissues. *Chem Rev*. 2003;103(2):577–644.
23. Verdier-Sévrain S, Bonté F. Skin hydration: a review on its molecular mechanisms. *J Cosmet Dermatol*. 2007;6(2):75–82.
24. Walsh JT Jr., Deutsch TF. Pulsed CO₂ laser tissue ablation: Measurement of the ablation rate. *Lasers Surg Med*. 1988;8(3):264–75.
25. Jansen ED, Leeuwen TGv, Motamedi M, Borst C, Welch AJ. Partial vaporization model for pulsed mid-infrared laser ablation of water. *J Appl Phys*. 1995;78(1):564–71.
26. Evers M, Ha L, Casper M, Welford D, Kosiratna G, Birngruber R, et al. Assessment of skin lesions produced by focused, tunable, mid-infrared chalcogenide laser radiation. *Lasers Surg Med*. 2018;50(9):961–72.
27. Ha L, Jaspán M, Welford D, Evers M, Kosiratna G, Casper MJ, et al. First assessment of a carbon monoxide laser and a thulium fiber laser for fractional ablation of skin. *Lasers Surg Med*. 2020;52(8):788–98.
28. Hibst R. Technik, Wirkungsweise und medizinische Anwendungen von Holmium-und Erbium-Lasern. *Fortschritte der Lasermedizin*: Ecomed-Verlag-Ges; 1997.
29. Lukac M, Vizintin Z, Kazic M, Sult T. Novel fractional treatments with VSP erbium YAG aesthetic lasers. *J Laser Health Academy*. 2008;2008(6):1–12.
30. Choi JE, Oh GN, Kim JY, Seo SH, Ahn HH, Kye YC. Ablative fractional laser treatment for hypertrophic scars: comparison between Er:YAG and CO₂ fractional lasers. *J Dermatol Treat*. 2014;25(4):299–303.
31. Preissig J, Hamilton K, Markus R. Current laser resurfacing technologies: a review that delves beneath the surface. *Semin Plast Surg*. 2012;26(03):109–16.
32. Avram MR, M AM, Friedman PM. *Laser and light source treatments for the skin*. Jaypee Brothers Medical Publishers Pvt. Limited; 2014.
33. Grunewald S, Bodendorf M, Illes M, Kendler M, Simon JC, Paasch U. In vivo wound healing and dermal matrix remodelling in response to fractional CO₂ laser intervention: Clinicopathological correlation in non-facial skin. *Int J Hyperthermia*. 2011;27(8):811–8.
34. Ciocon DH, Hussain M, Goldberg DJ. High-fluence and high-density treatment of perioral rhytides using a new, fractionated 2,790-nm ablative erbium-doped yttrium scandium gallium garnet laser. *Dermatol Surg*. 2011;37(6):776–81.
35. Ross EV, Swann M, Soon S, Izadpanah A, Barnette D, Davenport S. Full-face treatments with the 2790-nm erbium:YSGG laser system. *J Drugs Dermatol*. 2009;8(3):248–52.
36. Chen KH, Tam KW, Chen IF, Huang SK, Tzeng PC, Wang HJ, et al. A systematic review of comparative studies of CO₂ and erbium:YAG lasers in resurfacing facial rhytides (wrinkles). *J Cosmet Laser Ther*. 2017;19(4):199–204.
37. Wenande E, Anderson RR, Haedersdal M. Fundamentals of fractional laser-assisted drug delivery: an in-depth guide to experimental methodology and data interpretation. *Adv Drug Deliv Rev*. 2020;153:169–84.
38. Skorczakowski M, Swiderski J, Pichola W, Nyga P, Zajac A, Maciejewska M, et al. Mid-infrared Q-switched Er:YAG laser for medical applications. *Laser Phys Lett*. 2010;7(7):498–504.
39. Kosiratna G, Hibst ML, Jaspán M, Welford D, Manstein D. Effects of deviation from focal plane on lesion geometry for ablative fractional photothermolysis. *Lasers Surg Med*. 2016;48(5):555–61.

How to cite this article: Wang-Evers M, Blazon-Brown AJ, Ha-Wissel L, Arkhipova V, Paithankar D, Yaroslavsky IV, et al. Assessment of a 3050/3200-nm fiber laser system for ablative fractional laser treatments in dermatology. *Lasers Surg Med*. 2022;54:851–860.

<https://doi.org/10.1002/lsm.23550>